Activity and Kinetics of Dissociation and Transfer of Amphotericin B from a Novel Delivery Form

Submitted September 26, 1999; Accepted: October 5,1999; Published: August 21, 1999.

Bradley Baas, Katie Kindt, Angela Scott, Jessica Scott, Peter Mikulecky, and Scott C. Hartsel
Department of Chemistry, University of Wisconsin-Eau Claire, Eau Claire, Wisconsin 54702

ABSTRACT Recently it has been demonstrated that moderate heat treatment of Amphotericin B/deoxycholate solutions (HAmB-DOC) leads to a therapeutically interesting supramolecular rearrangement that can be observed by significant changes in light scattering, CD, and absorbance. In this study, we continue the investigation of the physical properties of this new form by evaluating the activity and kinetics of dissociation and dispersion of HAmB-DOC and AmB-DOC in saline, serum, and in model mammalian or fungal lipid biomimetic membrane vesicles. Stopped-flow spectrophotometry combined with singular value decomposition (SVD) and global analysis were used to resolve the components of this process. The dissociation kinetics for both states are complex, requiring multi-exponential fits, yet in most cases SVD indicates only two significant changing species representing the monomer and the aggregate. The kinetic mechanism could involve dissociation of monomers from coexisting spectroscopically similar but structurally distinct aggregates or sequential rearrangements in supramolecular structure of aggregates. Rate constants and amplitudes of dissociation from aggregates to monomer in buffer, whole serum, 10% cholesterol, and ergosterol membrane vesicles are generally greater for AmB-DOC, demonstrating its greater kinetic instability. In addition, at comparable low concentrations, HAmB-DOC and AmB-DOC are nearly equally active at promoting cation selective permeability in ergosterol-containing membranes; however, HAmB-DOC is much less active against mammalian mimetic cholesterol-containing vesicles, despite a higher level of self-association, supporting previous observations that there exists a specific "toxic aggregate" structure.

Abbreviations AmB, Amphotericin B; AmB-DOC, Amphotericin B/deoxycholate 5:4 (wt/wt) mixture; HAmB-DOC, Amphotericin B/deoxycholate 5:4 mixture heat-treated; LUV, large unilamellar vesicle(s); SUV, small unilamellar vesicle(s); FCCP, carbonyl cyanide p- (trifluoromethoxy) phenylhydrazone; egg PC, egg phosphatidylcholine; HDL, high density lipoproteins; LDL, low density lipoproteins.

INTRODUCTION

Amphotericin B (AmB) is a polyene macrolide antibiotic used to effectively combat systemic fungal infections, yet its utilization as an antifungal agent is inhibited by high acute and chronic toxicity, characterized by chills, fever, nausea, vomiting, and nephrotoxicity (1-3). AmB's selectivity for fungi is thought to hinge on its enhanced ability to form ion channels in ergosterol-rich fungal membranes versus mammalian cholesterol-rich membranes. Nonetheless, AmB can also damage mammalian membranes by a similar mechanism, causing the host of serious side effects observed. Newer liposomal and lipid-associated drug delivery mixtures have been developed and tested and seem to reduce the drug's toxicity by reducing the concentration of free AmB in solution to below a certain threshold. When AmB in solution is below the threshold of AmB self-association, toxicity against fungi is still observed but human toxic effects decline (see (1,3) for a recent review). In the current model of AmB selective toxicity, soluble monomeric AmB is very active toward ergosterol-containing membranes, but a soluble self-associated oligomer damages sterol-free and cholesterol-containing membranes (4,5). In addition, the oligomer seems to be more susceptible to autooxidation, which may enhance its toxicity (6-8).

Three lipid-associated pharmaceutical preparations are currently on the market: AmBisome (Fujisawa Healthcare, Deerfield, IL), Amphotec (Alza, Palo Alto, CA), and Abelcet (Liposome, Princeton, NJ). They are fundamentally different physically: AmBisome is a true closed liposomal bilayer preparation, Amphotec is a micellar solution with cholesteryl sulfate, and Abelcet is an interdigitated lipid dispersion (1). Despite these differences, they all possess a far superior therapeutic index to the original micellar commercial preparation consisting of AmB: deoxycholate (AmB-DOC) in a mole ratio of ~1:2 (Fungizone; Bristol Myers-Squibb, Princeton, NJ) (2). As promising as these new preparations are, their universal adoption may be

Corresponding Author: Scott C. Hartsel, Department of Chemistry, Phillips 461, University of Wisconsin-;Eau Claire, Eau Claire, Wisconsin 54702-4004; telephone: (715) 836-4746; facsimile: (715) 836-4979; e-mail: hartsesc@uwec.edu

hampered by their great expense, particularly in the Third World, where AIDS-related fungal infections are rampant. As a potential simple and inexpensive alternative, Bolard and Gaboriau (8,9) have discovered that AmB or AmB-DOC solutions may be treated with moderate heat (70°C for 20 minutes) to produce a new self-associated state of AmB, the "superaggregate," which we will refer to as heat-treated AmB-DOC (HAmB-DOC). This new species is spectroscopically distinct from AmB-DOC, with a blue-shifted absorption maximum and characteristic CD spectrum. This preparation has been shown to be much less cytotoxic in vitro. In addition, hemolysis, usually used as an indicator of potential human toxicity, is strongly inhibited by this heat treatment process. In model murine infections, HAmB-DOC has recently been shown to have a superior therapeutic index (10). This superaggregate species is fascinating both for the possible practical therapeutic benefits and for its potential for explaining the root mechanisms for toxicity reduction in the simplest possible improved Amphotericin B drug delivery system. In this report, we continue the investigation of the physical properties of this new form by evaluating the kinetics of dissociation and dispersion of HAmB-DOC and AmB-DOC in saline, serum, and in model lipid membrane vesicles. Stopped-flow and singular value decomposition (SVD) and global analysis were used to resolve the components of this process. In addition, we directly compare the abilities of these two forms to induce ion channels in model fungal and mammalian mimetic membrane systems.

MATERIALS AND METHODS

Materials

All lipids were purchased from Avanti Polar Lipids (Alabaster, AL). Purified Amphotericin B was a generous gift from Bristol-Myers Squibb Pharmaceuticals (Princeton, NJ). AmB-DOC as Fungizone (Bristol-Myers Squibb Pharmaceuticals) was purchased from a commercial supplier. FCCP (carbonyl cyanide p- (trifluoromethoxy) phenylhydrazone), cholesterol, and ergosterol were obtained from Sigma Chemical (St. Louis, MO). The sterols were recrystallized from ethanol 3X before use. Valinomycin, a K+ ionophore, was purchased from CalBiochem (La Jolla, CA). Laser-grade pyranine (1,3,6-pryrenetrisulfonic acid) was purchased from Eastman-Kodak (Rochester, NY). Whole bovine serum was obtained from Sigma Chemical and had to be diluted 6:1 in PBS due to the high absorbance of the serum between 300 and 400 nm.

HAmB-DOC was made by heating a 100 mM (in AmB) solution of Fungizone dissolved in phosphate buffered saline (PBS; 155 mM NaCl, 7mM Na2HPO4, 3 mM KH2PO4, pH 7.4) to 70°C in water bath for 20 minutes. AmB-DOC stocks were removed from the same preparation before heating. Both preparations were purged with argon and kept in darkness to prevent oxidation. In order to determine whether the heating may have caused chemical as well as physical changes in the AmB, HPLC and absorption spectroscopy were used. Briefly, aliquots of AmB-DOC and HAmB-DOC were diluted 10:1 into methanol for spectroscopy or into acetonitrile for HPLC analysis. Absorbance spectral peaks of both preparations in methanol were identical within the 0.2-nm resolution of the Cary-14 spectrophotometer and the intensities changed < 5% after heating. Gradient reversed-phase HPLC (Poros R2 medium; PerSeptive Biosystems, Framingham, MA) using a 20-60% water/acetonitrile gradient showed only a single peak at 415 nm, with identical retention times for both preparations. The two most likely chemical modifications of AmB upon heating would be oxidation of the polyene backbone or cleavage of the lactone ring. The former would lead to a disappearance or serious alteration of the characteristic methanol spectrum, and the latter would be expected to alter the retention time by HPLC. Since neither of these methods showed a significant change for AmB properties after heating, it is a reasonable assumption that the differences observed here are due solely to supramolecular structure changes.

Preparation and Assay of Lipid Vesicle Samples for Ion Permeability and Binding Studies

The lipids were dispersed in a 15 mM K2HPO4, 2 mM pyranine buffer with 200 mM KCl at pH 7.20 for ion permeability studies or in PBS for kinetic dilution and distribution studies. The lipid dispersions were then freeze-thawed and extruded ten times through 200 nm (with Lipex unit only) followed by 100 nm Nucleopore filters using a pressure (Lipex, Vancouver, BC) or manual (Avanti Polar Lipids) extruder to make large unilamellar

vesicles (LUV) of ca. 100 nm diameter. Where present, the external pyranine solution was removed and exchanged with a 15-mM K2HPO4 osmotically balanced (with sucrose) buffer through gel filtration with Sephadex G-25, thus forming a (K+) gradient of 6.67 K+in /K+ out across the membrane. 3 mM FCCP was added to pyranine-containing vesicles to allow for free equilibration of H+ ions.

Measurement of K+, Cl-, and Net Ion Currents in LUV

Ion currents were measured by fluorescence with an Applied Photophysics SX.18MV stopped-flow spectrophotometer with a 500-nm cutoff filter in place. Stopped-flow techniques for measuring ion currents using the pH sensitive dye pyranine as a reporter molecule have been developed over the past few years, and the concentrations, data handling, interpretation, and other experimental conditions were essentially identical to those in Ruckwardt et al. (11). For the current studies, HAmB-DOC and AmB-DOC were introduced to vesicles from a buffer identical to the column exchange buffer via stopped flow syringes of 1:11 or 1:26 dilution ratios to the final concentrations at thermostatted temperature (37.0 ± 0.5°C). The final total lipid concentration was 1.1 mg/ml. Our assay measures pH changes inside the LUV that result from the AmB induced net K+ currents. The net flux of K+ (or any ion) across a membrane vesicle is electrogenic, i.e., it generates a transmembrane voltage that can be approximated by the Nernst equation if perfect selectivity is seen. The incorporation of the protonophore FCCP into the LUV allows H+ to move rapidly across the membrane, and it will quickly come to equilibrium with this transmembrane voltage. The imposed salt gradients coupled with the ionophoric action of AmB lead to an H+ for K+ (or Cl-) exchange that is limited by the rate of AmB induced K+ or Cl- efflux. Under our conditions, according to the Nernst equation, ideal K+ selectivity at low buffer capacity should produce a final pH difference of -0.82. The pyranine molecules entrapped in the target LUV provide a sensitive fluorescence assay for detecting this resulting interior vesicular pH change. The fluorescence intensity of the pyranine is linear between about 7.8 and 6.4, and so fluorescence intensity was converted directly to internal pH. Hence, these amphotericin-induced ion currents can be observed as a dynamic change in pH, and AmB membrane activity is reported as change in pH/second. In the present experimental configuration, a fluorescence decrease indicates K+ > Cl- selectivity and an increase would follow from Cl- > K+ selectivity. In each case, a baseline fluorescence change of LUV in the absence of AmB was subtracted from the data to rule out nonspecific defects and leaks as a source of the observed change in fluorescence. The K+ ionophore valinomycin was used as a perfectly K+ selective control. In all cases, AmB produced cation selective channels/defects (fluorescence decrease) close to expected Nernst potentials.

Measurement of Absorption and CD Kinetics and Steady-State Spectra and Data Analysis

Kinetic photodiode array spectral series were taken using a microvolume stopped-flow reaction analyzer (Applied Photophysics, U.K., and SX.18MV). Spectral series were measured at 37°C from 300 to 450 nm using a diode array detector with an integration time of 10.080 ms. The mixing chamber had a 1.0-cm pathlength, and a monochrometer slit width was generally fixed at 0.5 mm entry and 0.2 mm exit. Oversampling was employed with a 200- or 500-second log time base. All samples were protected from light to prevent photo-oxidation of AmB. SVD and global analysis software from Applied Photophysics was used for data analysis. Steady-state CD spectra were taken using the Applied Photophysics CD attachment.

SVD analysis can be used to suggest a minimum number of species contributing to a spectral family (12,13). As an example of this process, we will inspect the time-dependent (200 seconds) spectral change of HAmB-DOC diluted 11:1 (100mM to 9.1 mM) into 10 mole percent ergosterol/egg PC LUV (total (lipid) = 1.1 mg/ml). The time dependent absorbance data matrix, A, can be decomposed into an output data matrix where A = USVT where V (see column 1, Figure 1) is the matrix of the time-dependent amplitudes and matrix U (see column 2, Figure 1)represents the basis spectra.

When the first several singular values (the diagonal matrix S, Figure 1, column 3) in a set of spectra are inspected, it is usually straightforward to estimate the rank of the data matrix A since the singular values will plateau. By inspection of the data in Figure 1, it can be concluded that there are only two significantly changing species. Hence a model-free assessment of the number of significantly contributing species in

the process can be obtained and the spectral noise can be reduced in the process of reconstitution of the spectral family. The reconstituted spectral family composed of the first two basis vectors only is shown in Figure 2, along with the raw data (inset).

The species represented as basis spectra are not necessarily distinct chemical species but may be linear combinations of spectra that improve the fit to the data. In all of the other spectral analyses, HAmB-DOC had only two significant (ascertained by their singular values) basis spectral vectors, which resembled the initial primarily self-associated form (S1) and a difference spectrum between this form and the monomer (S2). AmB-DOC spectral families occasionally demonstrated a third species that was small but significant. This may be indicative of the auto-oxidation process due to the greater propensity of AmB-DOC to photo- and air oxidize as compared to HAmB-DOC (see below and (8)). Because our samples were degassed and purged with argon, photo-oxidation is the most likely contributor.

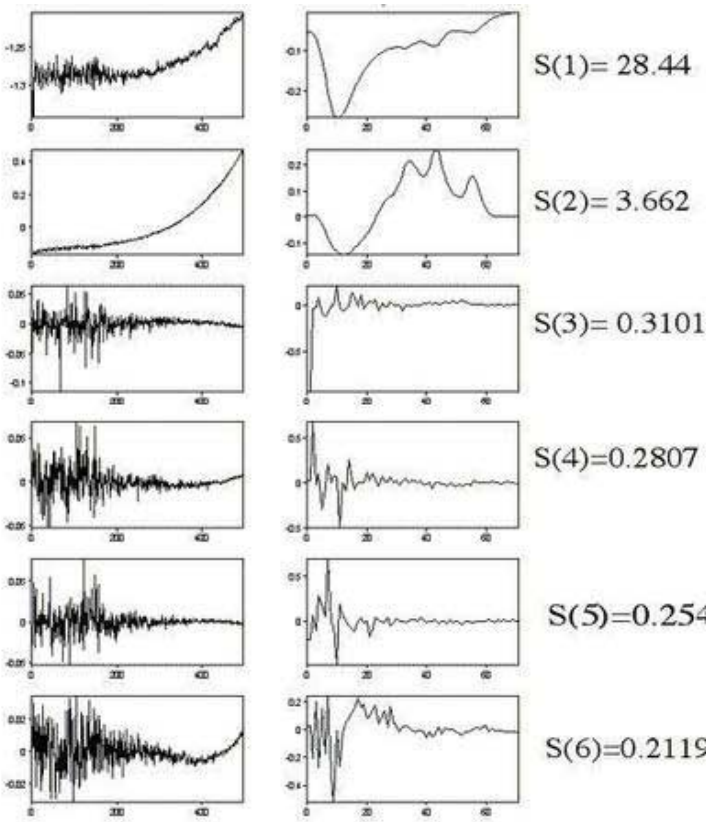

Figure 1. The first six singular value decomposition vectors for the time dependent amplitude, column 1, *x* axes = time (seconds), *y* axes = amplitude of the corresponding basis spectrum; basis spectra, column 2, *x* axes = wavelength units (nm), *y* axes = absorption amplitudes of the independent basis spectra; and singular values, column 3, diagonal matrix elements that describe the magnitudes of the contributions of the outer products of the previous column vectors. These values were obtained from an SVD of a spectral family gathered from the time-dependent redistribution of 100 mM HAmB-DOC diluted 11:1 into 1.1 mg/ml LUV composed of 10 mole percent ergosterol/egg PC at 37°C.

RESULTS

As shown previously, we observed a marked blue shift of the absorption maximum of AmB-DOC to ~320 nm from ~330 nm after heat treatment (8,9). The CD spectra (data not shown) showed a weak bilobed band that also shifted correspondingly, demonstrating complete or nearly complete conversion of AmB-DOC to HAmB-DOC.

Sample Oxidation

One concern with diode array detection systems is that potentially light sensitive samples are exposed continuously to a broad spectrum of a 150-watt xenon lamp source. Because Amphotericin B is light and oxygen sensitive and susceptible to autooxidation, we looked at light sensitivity in our system under relatively harsh conditions. With our light source slits open to 0.50 mm (before the fiber optic light guide) and no attempt to remove dissolved oxygen from the samples, a significant amount of photo and/or air oxidation was observed with both HAmB-DOC and AmB-DOC (Figure 3a,b) over the course of a 500-second exposure.

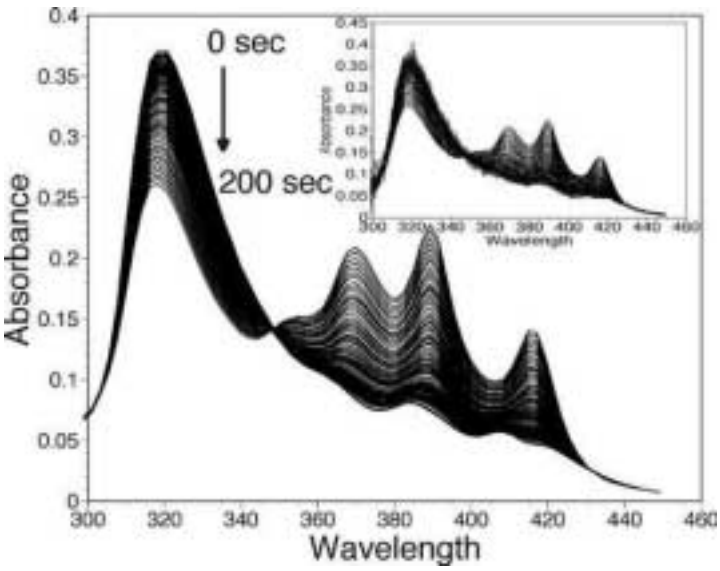

Figure 2. Reconstituted spectra of HAmB-DOC redistribution corresponding to the first two vectors for the SVD in Figure 1. Inset is the raw data output collected logarithmically from 0.005 to 200 seconds from the stopped-flow diode array detector.

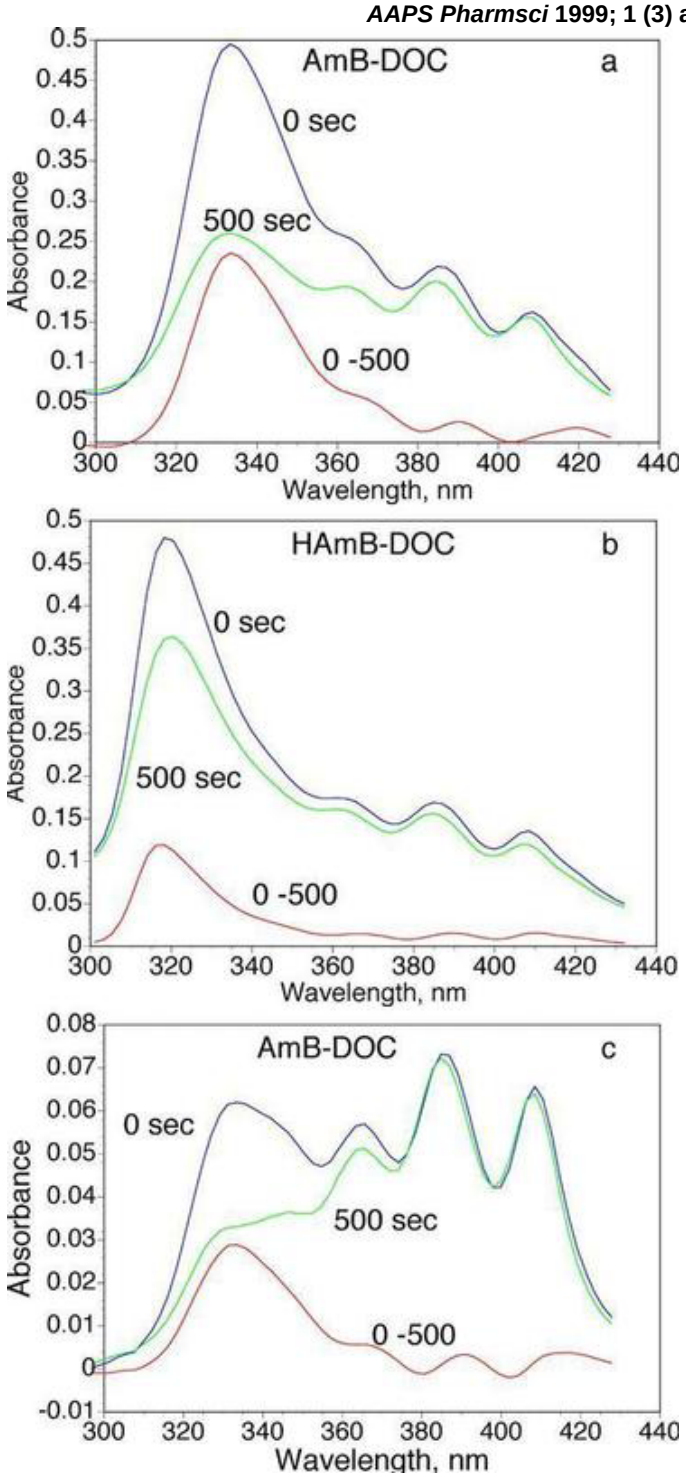

Figure 3. Photo and air oxidation loss of Amphotericin B from the two drug delivery systems. No attempt was made to remove dissolved oxygen or minimize light exposure. a) t = 0 seconds and t = 500-second spectra and difference spectrum of AmB-DOC, 9.1 µ'b5M, 1 cm pathlength, 0.5 mm optical slit exposed to a 150-W Xenon lamp output; b) t = 0 seconds and t = 500-second spectra and difference spectrum of HAmB-DOC, 9.1 µM, 1 cm pathlength, 0.5 mm optical slit exposed to a 150-W Xenon lamp output; c) t = 0 seconds and t = 500-second spectra and difference spectrum of AmB-DOC, 1.6 µM, 1 cm pathlength, 0.5 mm optical slit exposed to a 150 W-Xenon lamp. Notice that in all three cases only the blue-shifted, self-associated form of AmB is lost, leaving behind the monomer.

However, as observed by Gaboriau (8), heat treatment provided some protection (24 vs. 48% lost for AmB-DOC) against drug oxidation. In addition, there are other interesting features to the difference spectra of the time = 0 - time = 500 seconds. The difference spectra absorption maximum corresponds closely to the maxima of the species' respective oligomer forms (Amax = ~319 nm and 333 nm for HAmB-DOC and AmB-DOC, respectively). Furthermore, even when diluted to a final (AmB) of 1.6 µM, where more monomer is present (Figure 3c), still only the oligomer is lost to oxidation.

This is consistent with previous results showing that an aggregated species undergoes an autooxidation process resulting in free radical formation (6,7). The fact that HAmB-DOC oxidation difference spectrum does not have a significant shoulder at 433 nm indicates that there is not a significant interconversion to the oxidation-sensitive self-associated species found in AmB-DOC. This implies that an AmB-DOC to HAmB-DOC transition is essentially irreversible. In practice, we found that degassing and saturating samples with argon, and reducing the optical slit width to 0.2 mm or less (which required an increase in the integration time to ~10 msec to obtain reasonable signal/noise) was adequate to prevent most degradation.

Kinetics and SVD of AmB Release and Redistribution

Kinetics and SVD of AmB release and redistribution upon dilution into our systems demonstrate complexity. The dissociation/redistribution spectral families obtained from the 1:11 and 1:26 dilutions could not be well fitted globally by a first-order process in any case. This is the case, despite the apparent presence of an isosebestic point in nearly all of the spectral families, which would normally suggest a simple two-species interconversion (e.g., dimer to monomer). In the global fitting procedure, the best fit was assumed to be the one with the smallest number of exponentials giving reasonable residuals. Where possible, it is preferable use a known basis spectrum to aid in the fit. A representative aqueous monomer spectrum was generated for this purpose by dilution of an AmB-DOC solution to 0.4 x 10-7 M and allowed to dissociate at 37°C until no further change in

absorbance at 409 nm was observed. This basis spectrum was used in cases where the absorption maxima of the evolving species were the same as the aqueous monomer. In addition, the 9.1 mM AmB-DOC was visually determined to dissociate nearly 100% into 10 mole percent ergosterol /eggPC vesicles into a new monomer-like species. This putative ergosterol-associated form has principal absorption transitions at 416, 389, 370, and 354 nm in contrast to transitions of 409, 385, 365, and 346 nm in the aqueous monomer. This basis spectrum was used in cases where the absorption maxima of the evolving species were the same as the ergosterol-associated monomer. In contrast, in the presence of 10 mole percent cholesterol-containing vesicles, there was no apparent unique cholesterol-bound species. Instead, the evolving spectrum was indistinguishable from the aqueous monomer as determined by its absorption maxima.

There are many potential kinetic models of AmB dissociation. We chose the following models for global fitting:

(1) A→M

(2) A→A2 [rarrow]]M

(3) A→A2→A3→M

(4) A→M
A2→M

(5) A→M
A2→M
A3→M

where A is an initial AmB aggregate, A2 is a different aggregate, A3 is a third type of aggregate, M is "monomer" (ergosterol-bound or free aqueous). Since all spectra were produced from rapidly diluted 100 µM AmB, the initial spectrum at time = ~10 msec reflected an aggregated species (8). The observed basis spectra generated by the global kinetic fits suggest a rapid conversion from one spectroscopically distinct aggregate state with a blue shifted peak to another similar one. Physically, this could represent the dissociation of large aggregates into smaller oligomeric units (minimum: dimer) or aggregates of different sizes and/or compositions with only slightly different spectra. In the case of AmB-DOC, for example, it has been show that micellar aggregates of polydisperse sizes and AmB:DOC ratios exist and develop with time upon reconstitution of the dried mixture (14).

As an example of the process, the dissociation/redistribution of AmB from the two delivery systems into fungal mimetic membrane vesicles (10 mole percent ergosterol/egg PC) is shown in Figures 4 and 5. The figures are global fitting-generated basis spectra, or wavelength dependent amplitudes (Figures 4a,5a) and concentration profiles over time of these species (Figures 4b,5b) generated from SVD-processed diode array data sets.

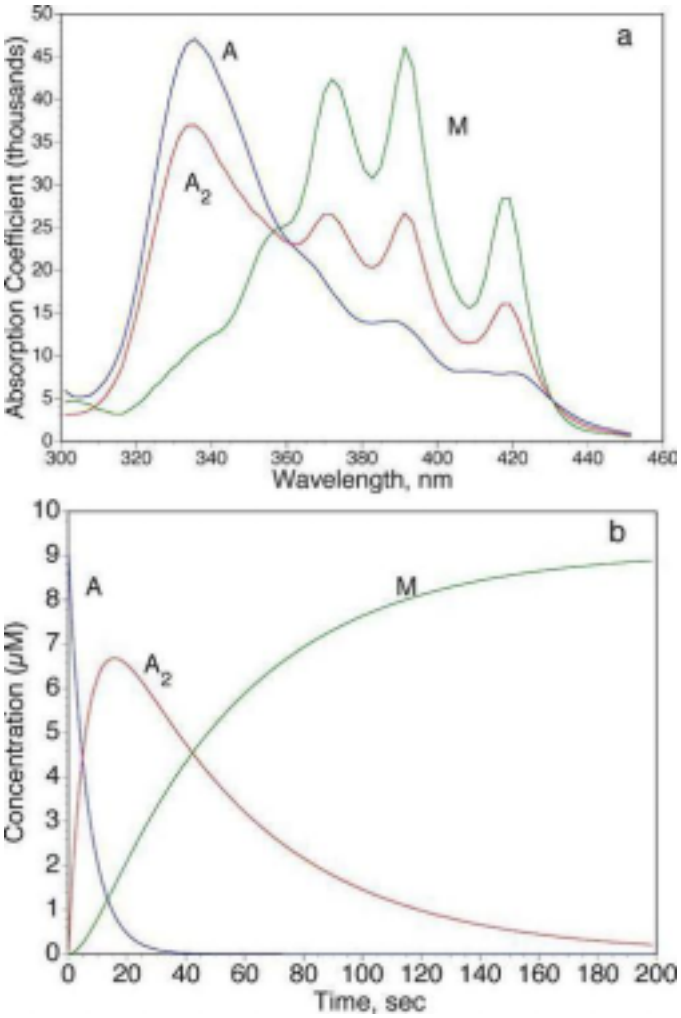

Figure 4. Basis spectra and concentration profiles produced from the Pro-K global fitting procedure of a 200-second data set produced from an 100-µM AmB-DOC solution diluted 11:1 into 1.1 mg/ml LUV composed of 10 mole percent ergosterol/egg PC at 37°C. The fit of the 3 SVD reconstituted spectra were fit to a sequential first-order scheme, A→A2→M, where A is the initial self-associated form of AmB-DOC, A2 is an intermediate state formed from A, and M is a constrained basis spectrum produced by complete association of AmB with ergosterol-containing LUV.

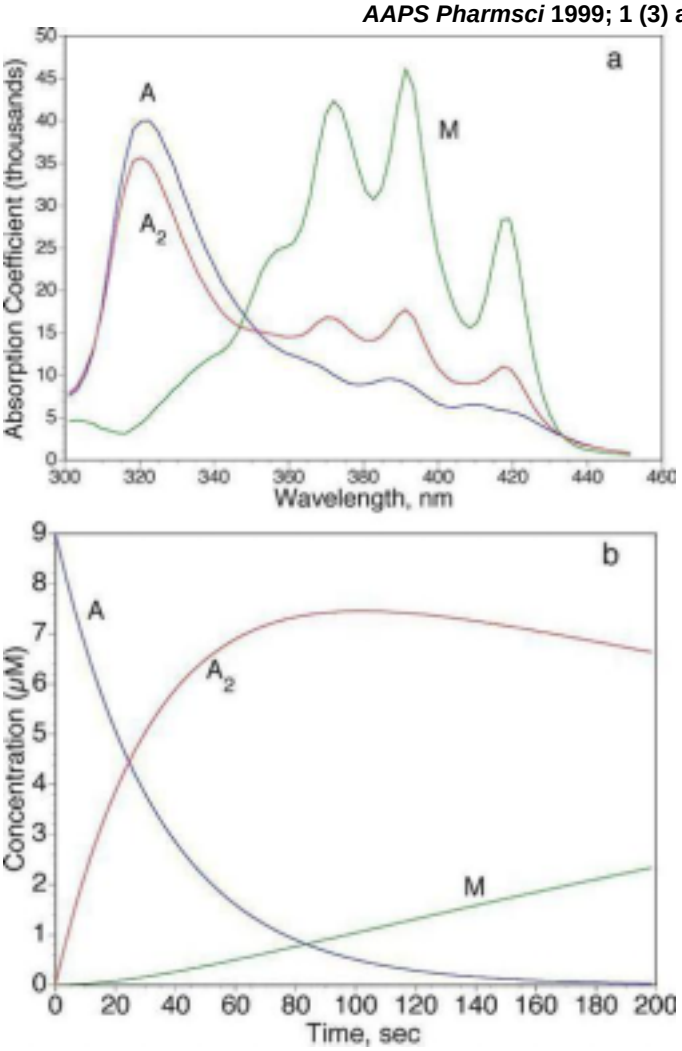

Figure 5. Basis spectra and concentration profiles produced from the global fitting of a 200-second data set produced from a 100-mM HAmB-DOC solution diluted 11:1 into 1.1 mg/ml LUV composed of 10 mole percent ergosterol/egg PC at 37°C. The fit of the two SVD reconstituted spectra were fit to a sequential first-order scheme, A→A2→M, where A is the initial self-associated form of HAmB-DOC, A2 is an intermediate state formed from A, and M is a constrained basis spectrum produced by complete association of AmB with ergosterol-containing LUV.

The set of data used for the analysis of the HAmB-DOC (Figure 5) is the same as that in Fig1. The global kinetic analysis fitted the data adequately with a sequential first-order reaction scheme A→A2→M, as shown in Figures 4 and 5, though marginal improvements in the residuals and variance could be made by including an additional component in a A→A2→A3→M type of scheme (not shown). The characteristic ergosterol-associated AmB spectrum was used as the target basis spectrum for "M" for both fits. In this way, direct comparison of the rate of production of an ergosterol-associated species could be made between HAmB-DOC and AmB-DOC. The

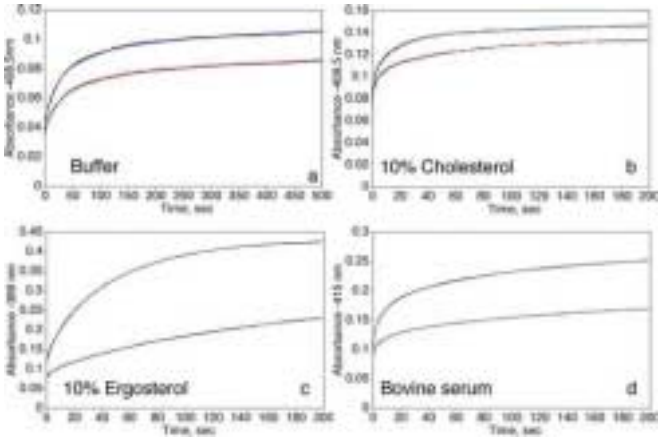

Figure 6. Examples of single-fitted kinetics to show the quality of the fit at the most intense monomer-like wavelength(s) are shown here. The four fits correspond to the four samples of AmB-DOC and HAmB-DOC globally fitted to obtain the data in {Table 1}==null1==((RECALL:Table1)). The blue lines correspond to AmB-DOC, while the red lines are HAmB-DFOC data. Black lines underlying these traces represent the individual fits. All data were collected at 37°C and pH 7.4. a) AmB-DOC and HAmB-DOC dissociating in buffer. Samples were rapidly diluted from 100 μM to 3.8 μM; b) AmB-DOC and HAmB-DOC dissociating in a suspension of 1.1 mg/ml LUV composed of 10 mole percent cholesterol/egg PC samples were rapidly diluted from 100 μM to 9.1 μM; c) AmB-DOC and HAmB-DOC dissociating in a suspension of 1.1 mg/ml LUV composed of 10 mole percent ergosterol/egg PC. Samples were rapidly diluted from 100 μM to 9.1 μM; d) AmB-DOC and HAmB-DOC dissociating into 6:1 diluted (with PBS) whole bovine serum. Samples were rapidly diluted from 100 μM to 9.1 μM.

Table 1. Rates of dissociation/redistribution of Amphotericin B (sec-1) introduced into various systems in a sequential first-order reaction global fit of the form A→A2→M. Principal absorption maxima for the "monomer-like" spectra are included. All spectra were reconstituted with two singular value components, except where indicated.

System	1:26 dilution into PBS buffer, fitted to buffer monomer basis spectrum	1:11 dilution into cholesterol-containing LUV fitted to buffer monomer basis spectrum	1:11 dilution into ergosterol-containing LUV fitted to ergosterol-monomer basis spectrum	1:11 dilution into calf serum (1:6 dilution) free global fit
AmB-DOC (fungi zone)	k1 = 0.0683 k2 = 0.000400 var = 0.00000262 l(nm) = 408, 385, 331	k1 = 0.0568 k2 = 0.00000240 var = 0.0000167 -3 SVD l(nm) = 408, 385, 332	k1 = 0.0876 k2 = 0.0193 var = 0.00000623 -3 SVD l(nm) = 416, 389, 370,353	k1 = 0.484 k2 = 0.0193 var = 0.00000328 l(nm) = 414, 388, 336
HAmB-DOC (Heated fungi zone)	k1 = 0.0873 k2 = 0.000565 var = 0.00000121 l(nm) = 408, 385, 318	k1= 0.104 k2 = 0.000207 var = 0.00000469 l(nm) = 408, 385, 319	k1= 0.0293 k2 = 0.00184 var = 0.00000352 l(nm) = 416, 389, 318	k1= 0.482 k2 = 0.0146 var = 0.00000144 l(nm) = 414, 388, 319

global fits show that transfer from the AmB-DOC aggregate to the ergosterol-associated form is much more rapid kinetically (essentially 100% after 200 seconds) than from the HAmB-DOC aggregate (~20% after 200 seconds). This demonstrates again the kinetic stability conferred by this simple heat treatment. Global fitting with parallel first-order reaction schemes such as (4) and (5) above produced unreasonable basis spectra (e.g., negative absorption coefficients) for either system.

Individual kinetic traces at the most intense monomer absorption transition wavelength for AmB-DOC and HAmB-DOC dissociation/redistribution and their fits (using kinetic model (2)) are shown in Figure 6a through 6d. In PBS buffer, rapid dilution of AmB-DOC and HAmB-DOC from 100 to 3.8 mM leads to a production of a typical AmB aqueous monomer with an absorption maximum of 408-409 nm (Figure 6a, Table 1).

Both processes could be adequately fitted by two sequential first-order reactions, with the final species, M, basis spectrum fixed as an aqueous monomer spectrum. The global fits for both yielded similar rate constants, with the rate-limiting step being the production of the free aqueous monomer. The major difference was the greater amplitude of the AmB-DOC system in this region, demonstrating the greater kinetic instability of the self-associated species of AmB in AmB-DOC. A similar process was observed for the dilution of AmB-DOC and HAmB-DOC from 100 to 9.1 mM in the presence of 1.1 mg/ml 10 mole percent cholesterol/egg PC LUV (Figure 6b).

The absorption maxima of the species generated were identical to the aqueous form of AmB and suggest little direct interaction with the cholesterol or the lipids. In contrast, as outlined above, there are major differences in the rate of redistribution as well as the resultant spectrum (Table 1) in the presence of 1.1 mg/ml 10 mole percent ergosterol/egg PC LUV, which indicate a strong and rapid interaction of AmB with ergosterol (especially from AmB-DOC) and essentially no free aqueous monomer in either (Figure 6c).

A major difference in the amplitude of the redistribution of AmB from these two systems is also apparent in Figure 6d, where the diluent is whole bovine serum previously diluted 1:6 with PBS.

This situation is most similar to the "real" environment of therapeutically used AmB, which is generally administered parenterally. It can be seen that "monomeric" AmB dissociates more rapidly from the AmB-DOC system than HAmB-DOC. The very distinct absorption maximum shift of the monomer-like state from the aqueous 408 nm to 414 nm suggests that AmB is protein or lipoprotein-bound.

Activity of AmB-DOC and HAmB-DOC Against Mammalian and Fungal Mimetic Membranes

The comparative activities of AmB-DOC and HAmB-DOC against 10 mole percent ergosterol and 10 mole percent cholesterol-containing egg PC membrane vesicles are shown in Figures 7 and 8. Not surprisingly, the AmB-DOC concentrations required to produce significant ion currents in ergosterol-containing vesicles were much lower than in cholesterol-containing vesicles (Figure 7).

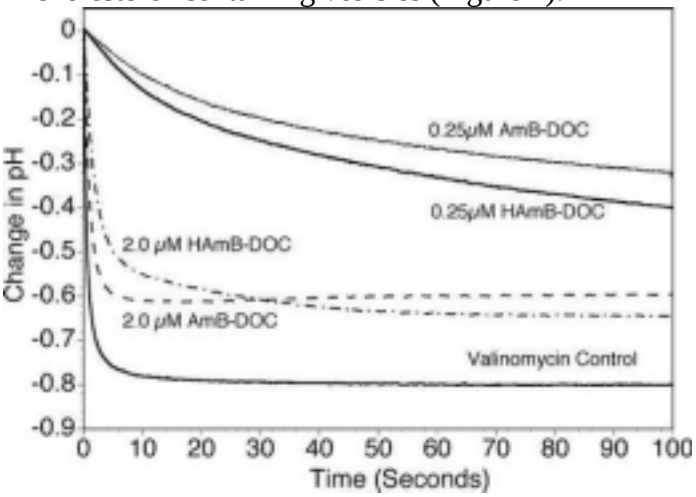

Figure 7. Fluorescence detected pH changes induced by AmB-DOC and HAmB-DOC in a suspension of 1.1 mg/ml LUV composed of 10 mole percent ergosterol/egg PC with a 6.67:1 K+ gradient. The decrease in fluorescence is due to K+/H+ exchange and demonstrates electrogenic K+ currents caused by AmB channel structures. The currents were detected for both systems at final (AmB) of 0.25 and 2.0 μM. The direction and magnitude of the antibiotic channel-mediated currents suggest a high degree of selectivity of K+ over Cl-. Valinomycin at 0.1 μM was used as a potassium-selective control.

This is consistent with the observation that monomeric AmB is primarily active against fungi and ergosterol-containing membranes, whereas a "soluble aggregate" form is thought to be most active against sterol-free and cholesterol-containing membranes and hence is most toxic toward mammalian cells (15). The most striking contrast between AmB-DOC and HAmB-DOC, however, is in their activities against cholesterol-containing membranes. At 2.0 mM, AmB-DOC and AmB made from a 1-mM DMSO stock showed considerable, K+ selective ion current activity (Figure 8).

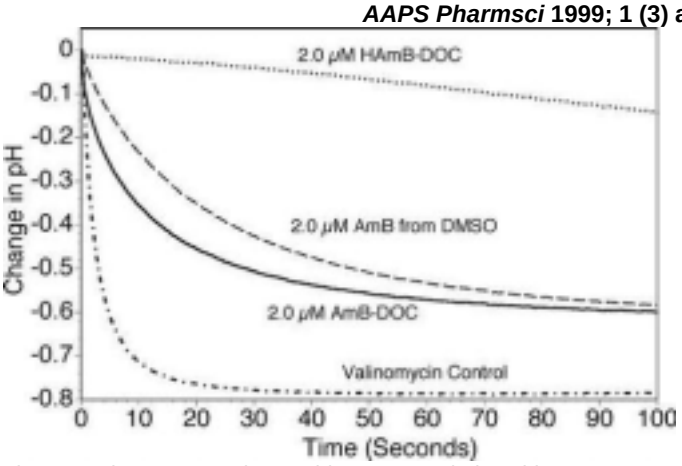

Figure 8. Fluorescence-detected ion currents induced by AmB-DOC, HAmB-DOC, and AmB from a 1-mM DMSO stock solution in a suspension of 1.1 mg/ml LUV composed of 10 mole percent cholesterol/egg PC with a 6.67:1 K+ gradient. The currents were detected for both systems at final (AmB) of 2.0 μM. The direction and magnitude of the antibiotic channel-mediated currents again demonstrates a high degree of selectivity for K+ over Cl-. Valinomycin at 0.1 μM was used as a potassium-selective control. In this experiment, a striking reduction in activity is noted for the HAmB-DOC preparation as compared to the other preparations.

In contrast, the same concentration of HAmB-DOC initially showed almost no activity and only after a considerable lag (>60 seconds) began to exhibit some modest activity. The differences were not nearly as great against the ergosterol-containing vesicles, especially at very low concentrations (0.25mM), where both preparations would be expected to be largely monomeric and hence equally active (8). If each extruded vesicle is assumed to be 100 nm in diameter, 0.25 mM amounts to only ~18 AmB molecules/vesicle. At progressively greater concentrations, the AmB-DOC became more active than HAmB-DOC, as one would expect from the kinetic results above.

DISCUSSION

AmB is an extremely effective antifungal drug, yet its use is severely restricted due to its high toxicity. In the quest to make AmB a more generally useful drug, many different pharmaceutical preparations have been made; all of which involve complexation of AmB in lipid or sterol salt mixtures having many different supramolecular structures. Recently, a comparative study of four AmB delivery systems was carried out by Legrand et al. (16). Short-term toxicity against fungi was associated with relative monomer release from a stable core supramolecular structure, but damage to red blood cells (and by implication, humans) was associated with a lack of thermodynamic stability and increased self-association at concentrations >1mM. The latter undesirable features are associated with solutions of AmB-DOC and AmB produced from solvent stocks. In fact, the water-soluble self-associated form of AmB has been identified as the culprit with red blood cell toxicity (5,15). The attractiveness of the HAmB-DOC systems lies in the fact that it seems to be the least complicated way to "repackage" AmB into a less toxic form. In fact, deoxycholate is not even necessary to produce this characteristic heat-treated form (8); it is merely convenient, as it is widely available as a commercial preparation (Fungizone).

We have observed several important features imparted by the heat treatment. HAmB-DOC dissociates into monomers or monomer-like species to a lesser extent and generally more slowly into all model systems as compared to AmB-DOC. There seem to be only two significantly changing species spectroscopically by model-independent analysis of the singular value decomposition of HAmB-DOC, whereas AmB-DOC sometimes has three significant components. The complexity of the kinetics, however, points to the probability that the HAmB-DOC is a heterogeneous or evolving preparation. There have been previous observations of AmB-DOC micelle kinetic instability, heterogeneity of composition, and polydispersity (6,14,17). These authors noted that almost immediately upon reconstitution of dry AmB-DOC, the aggregate size steadily increased over a period of ~10 hours. Longer incubation revealed that gelatinous aggregates consisted largely of AmB, whereas the DOC remained wholly in solution. It is possible that our heat treatment accelerates this process of dissociation of AmB-DOC micelles followed by reassociation of AmB molecules. Stock solution solvents, concentrations, and compositions have also been shown to influence the size and nature of AmB self-associated species (5).

Despite the enhanced kinetic stability of the HAmB-DOC self-associated species, we have shown that the preparation still retains nearly as much K+ selective ion channel activity against ergosterol-containing targets (Figure 7), especially at concentrations less than 1 mM of total AmB, where the monomeric form of both preparations predominates (8). The monomeric state of AmB has previously been shown to be optimally selective for ergosterol binding when

dispersed in large amounts of DOC or when monomeric in the aqueous phase with monolayers (18,19). In contrast, the HAmB-DOC preparation at higher concentrations is much less active against cholesterol containing targets (Figure 8). This last observation is important mechanistically because more of the HAmB-DOC than AmB-DOC is expected to be present in a self-associated form. There is considerable evidence that AmB is most active against cholesterol-containing or sterol-free membranes through the action of a specific soluble self-associated form (4,5). It is clear then that this particular oligomeric form produced by heat treatment does not have this propensity and does not appreciably reconvert to the toxic soluble oligomer.

The interactions of these two preparations with serum is most interesting pharmaceutically because it more accurately reflects their condition upon therapeutic introduction to a subject. As with ergosterol-containing membranes, there is a markedly increased extent of monomerization with AmB-DOC, but the monomeric state seems to be protein and/or lipoprotein associated, as indicated by the spectral redshift (Table 1). A contributing factor to this enhanced "disassembly" of the AmB-DOC complex may be the known affinity of cholate and deoxycholate for serum albumin (20-22). AmB itself is also known to have at least two binding sites to albumin (23). Whatever the specific location(s) of the bound monomer-like species, there is no spectroscopic evidence in either the case of the AmB-DOC or HAmB-DOC that a significant fraction of aqueous monomer exists even in the presence of dilute serum. In fact, a recent surface-enhanced Raman study has shown that even at 10 -5 M AmB in serum there is less than 10-8 M of free monomeric AmB in solution (24). In light of this, the ion permeability results in Figures 7 and 8 in the absence of serum must be evaluated carefully when extrapolating to AmB toxicity/efficacy in animal disease models (25,26). Because there is probably no appreciable soluble monomer in a real system, the mechanism of toxicity against fungi and toxic effects against host cells must involve differential AmB transfer by contact with or uptake of proteins and/or lipoproteins by host cells. In fact, it has been shown in an endothelial cell culture system that the presence of calf serum can actually be protective against direct cellular membrane injury by AmB (27).

It has long been known that AmB associates extensively and rapidly with serum lipoproteins and proteins (28). In fact, due to the high relative concentrations of serum protein to lipoprotein, a major fraction of AmB (not AmB-DOC) was shown to be protein rather than lipoprotein associated (28). Different liposomal or micellar formulations of AmB have different distribution profiles in HDL vs. LDL fractions. There is a strong correlation between the binding of AmB to different lipoprotein fractions and human toxicity. The extent of binding to lipoproteins is associated with many additional factors, such as cholesterol content and diet history (29). It appears that the AmB delivery systems that bind primarily to LDL are generally more toxic to humans than those that bind to HDL, possibly due to systemic uptake via the LDL receptor (30-32,33). All of this suggests that the complete story of the improvement of therapeutic index with heat-induced resculpting of AmB aggregates probably involves changes in distribution into and interaction with various serum fractions, as well as the intrinsic reduction of activity against cholesterol-containing membranes. These differential interactions will be the subject of a future report.

ACKNOWLEDGEMENT

This work was supported by the National Science Foundation (MCB-9603582).

REFERENCES

1. Hartsel, S. and J. Bolard, Amphotericin B: new life for an old drug. Trends Pharmacol Sci. 1996;17:445-449.

2. Hiemenz, J.W. and T.J. Walsh, Lipid formulations of amphotericin B: recent progress and future directions. Clin Infect Dis. 1996;22:133-144.

3. Brajtburg, J. and J. Bolard, Carrier effects on biological activity of amphotericin B. Clin Microbiol Rev. 1996;9:512-531.

4. Bolard, J., P. Legrand, F. Heitz, and B. Cybulska, One-sided action of amphotericin B on cholesterol-containing membranes is determined by its self-association in the medium. Biochemistry. 1991;30:5707-5715.

5. Legrand, P., E.A. Romero, B.E. Cohen, and J. Bolard, Effects of Aggregation and Solvent on the Toxicity of Amphotericin-B to Human Erythrocytes. Antimicrob Agents Chemother. 1992;36:2518-2522.

6. Lamy-Freund, M.T., V.F.N. Ferreira, A. Faljonialario, and S. Schreier, Effect of Aggregation on the Kinetics of Autoxidation of the Polyene Antibiotic Amphotericin-B. J Pharm Sci. 1993;82:162-166.

7. Lamy-Freund, M.T., V.F. Ferreira, and S. Schreier, Mechanism of

inactivation of the polyene antibiotic amphotericin B. Evidence for radical formation in the process of autooxidation. J Antibiot (Tokyo). 1985;38:753-757.

8. Gaboriau, F., M. Cheron, L. Leroy, and J. Bolard, Physico-Chemical properties of the heat-induced 'superaggregates' of amphotericin B. Biophysical Chemistry, 1997;66:1-12.

9. Gaboriau, F., M. Cheron, C. Petit, and J. Bolard, Heat-induced superaggregation of amphotericin B reduces its in vitro toxicity: a new way to improve its therapeutic index. Antimicrob Agents Chemother. 1997;41:2345-2351.

10. Petit, C., V. Yardley, F. Gaboriau, J. Bolard, and S.L. Croft, Activity of a heat-induced reformulation of amphotericin B deoxycholate (fungizone) against Leishmania donovani [In Process Citation]. Antimicrob Agents Chemother.1999;43:390-392.

11. Ruckwardt, T., A. Scott, J. Scott, P. Mikulecky, and S.C. Hartsel, Lipid and stress dependence of amphotericin B ion selective channels in sterol-free membranes. Biochim Biophys Acta. 1998;1372:283-288.

12. Henry, E.R.a.H., J., Singular Value Decomposition: Application to Analysis of Experimental Data, in Numerical Computer Methods, L.a.J. Brand, M. L., Editor. 1992, Academic Press, Inc.: p. 129-192.

13. Fujii, G., J.E. Chang, T. Coley, and B. Steere, The formation of amphotericin B ion channels in lipid bilayers. Biochemistry. 1997;36:4959-4968.

14. Lamy-Freund, M.T., S. Schreier, R.M. Peitzsch, and W.F. Reed, Characterization and time dependence of amphotericin B: deoxycholate aggregation by quasielastic light scattering. J Pharm Sci. 1991;80:262-2666.

15. Hartsel, S.C., C. Hatch, W. Ayenew, How Does Amphotericin B Work? :Studies on Model Systems. Journal of Liposome Research. 1993;3:377-408.

16. Legrand, P., M. Cheron, L. Leroy, and J. Bolard, Release of amphotericin B from delivery systems and its action against fungal and mammalian cells. Journal of Drug Targeting. 1997;4:311-319.

17. Lamy-Freund, M.T., V.F. Ferreira, and S. Schreier, Polydispersity of aggregates formed by the polyene antibiotic amphotericin B and deoxycholate. A spin label study. Biochim Biophys Acta. 1989;981:207-212.

18. Barwicz, J. and P. Tancrede, The effect of aggregation state of amphotericin-B on its interactions with cholesterol- or ergosterol-containing phosphatidylcholine monolayers. Chem Phys Lipids. 1997;85:145-155.

19. Tancrede, P., J. Barwicz, S. Jutras, and I. Gruda, The effect of surfactants on the aggregation state of Amphotericin B. Biochim Biophys Acta. 1990;1030:289-95.

20. Ceryak, S., B. Bouscarel, and H. Fromm, Comparative binding of bile acids to serum lipoproteins and albumin. J Lipid Res. 1993;34:1661-1674.

21. Meyuhas, D. and D. Lichtenberg, The effect of albumin on the state of aggregation and phase transformations in phosphatidylcholine-sodium cholate mixtures. Biochim Biophys Acta. 1995;1234:203-213.

22. Passing, R. and D. Schubert, The binding of deoxycholic acid to band 3 protein from human erythrocyte membranes and to bovine serum albumin. Hoppe Seylers Z Physiol Chem. 1983;364:219-226.

23. Romanini, D., B. Farruggia, and G. Pico, Absorption and fluorescence spectra of polyene antibiotics in the presence of human serum albumin. Biochem Mol Biol Int. 1998;44:595-603.

24. Ridente, Y., J. Aubard, and J. Bolard, Absence in amphotericin B-spiked human plasma of the free monomeric drug, as detected by SERS. FEBS Lett. 1999;446:283-286.

25. Petit, C., V. Yardley, F. Gaboriau, J. Bolard, and S.L. Croft, Activity of a heat-induced reformulation of amphotericin B deoxycholate (fungizone) against Leishmania donovani. Antimicrob Agents Chemother. 1999;43:390-392.

26. Petit, C., M. Cheron, V. Joly, J.M. Rodrigues, J. Bolard, and F. Gaboriau, In-vivo therapeutic efficacy in experimental murine mycoses of a new formulation of deoxycholate-amphotericin B obtained by mild heating [In Process Citation]. J Antimicrob Chemother. 1998;42:779-785.

27. Cutaia, M., S.R. Bullard, K. Rudio, and S. Rounds, Characteristics of Amphotericin-B Induced Endothelial Cell Injury. J Lab Clin Med. 1993;121:244-256.

28. Brajtburg, J., Elberg, S., Bolard, J., Kobayashi, G. S., Levy, R. A., Ostlund, R. E., Jr., Schlessinger, D. and G. Medoff, Interaction of plasma proteins and lipoproteins with amphotericin B. J Infect Dis. 1984;149:986-997.(1) Brajtburg, J., Elberg, S.

29. Chavanet, P., V. Joly, D. Rigaud, J. Bolard, C. Carbon, and P. Yeni, Influence of Diet on Experimental Toxicity of Amphotericin B Deoxycholate. Antimicrob Agents Chemother. 1994;38:963-968.

30. Vertut-Doi, A., S.I. Ohnishi, and J. Bolard, The endocytic process in CHO cells, a toxic pathway of the polyene antibiotic amphotericin B. Antimicrob Agents Chemother. 1994;38:2373-2379.

31. Wasan, K.M., R.E. Morton, M.G. Rosenblum, and G. Lopez-Berestein, Decreased toxicity of liposomal amphotericin B due to association of amphotericin B with high-density lipoproteins: role of lipid transfer protein. J Pharm Sci. 1994;83:1006-1010.

32. Wasan, K.M. and G. Lopezberestein, The interaction of liposomal amphotericin B and serum lipoproteins within the biological milieu. J Drug Target. 1994;2:373-380.

33. Wasan, K.M. and J.S. Conklin, Enhanced amphotericin B nephrotoxicity in intensive care patients with elevated levels of low-density lipoprotein cholesterol. Clin Infect Dis. 1997;24:78-80.